

Biocidal Organotin Compounds. Part 2. Synthesis, Characterization and Biocidal Properties of Triorganotin(IV) Hydantoic Acid Derivatives and the Crystal Structures of Triphenyltin and Tricyclohexyltin Hydantoates

S. K. Kamruddin,* T. K. Chattopadhyaya,* A. Roy* and E. R. T. Tiekink†‡

* Department of Chemistry, University of North Bengal, Darjeeling-734430, India, and † Department of Chemistry, The University of Adelaide, Adelaide, South Australia 5005, Australia

The preparation and spectroscopic (^1H NMR, UV and IR) characterization of three $\text{R}_3\text{Sn}(\text{O}_2\text{CCH}_2\text{N}(\text{H})\text{C}(\text{O})\text{NH}_2)$ [$\text{R}=\text{Ph}$, *c*-Hex (cyclohexyl) or *n*-Bu] compounds are reported. A different mode of coordination is indicated for the hydantoate ligand in the $\text{R}=\text{Ph}$ compound compared with the $\text{R}=\text{c}$ -Hex and $\text{R}=\text{n}$ -Bu compounds, as confirmed by a crystallographic analysis. The structure of $[\text{Ph}_3\text{Sn}(\text{O}_2\text{CCH}_2\text{N}(\text{H})\text{C}(\text{O})\text{NH}_2)]$ is polymeric owing to the presence of bridging hydantoate ligands such that each ligand coordinates one tin atom, via one of the carboxylate oxygen atoms, and a symmetry-related tin atom via the carbonyl group at the other end of the molecule. The structure features distorted trigonal-bipyramidal tin atom geometries with a *trans*- R_3SnO_2 motif. The structure of $[\text{c-Hex}_3\text{Sn}(\text{O}_2\text{CCH}_2\text{N}(\text{H})\text{C}(\text{O})\text{NH}_2)]$, by contrast, is monomeric, distorted tetrahedral, as the carboxylate group is monodentate and there are no additional tin–ligand interactions. The structures are each stabilized by a number of intermolecular hydrogen bonds. Fungitoxicity and phytotox-icity studies indicate that the $\text{R}=\text{n}$ -Bu derivative is the more active compound.

Keywords: triorganotin; carboxylate; crystal structure; fungitoxicity

INTRODUCTION

Various triorganotin carboxylates are known to have significant biocidal properties^{1,2} and it is expected that the incorporation of biologically active entities into a triorganotin system would lead to the formation of potent biocides. Hydantoic acid, $\text{H}_2\text{NC}(\text{O})\text{N}(\text{H})\text{CH}_2\text{C}(\text{O})\text{OH}$, and some of its derivatives are known to possess biological activity³ and, in the above context, its reactions with triorganotin moieties have been investigated in the present study. In addition to the carboxylate binding site, the anion derived from hydantoic acid has other potential donor sites available for coordination. As a continuation of previous work on the structure–activity relationship of organotin(IV) carboxylates,⁴ the present report details a study of the interaction of triorganotin centres with hydantoic acid employing spectroscopic and crystallographic methods, and describes some biocidal properties of the new compounds.

EXPERIMENTAL

General

The solvents were purified and dried by standard procedures before use. Ph_3SnCl , $(\text{n-Bu}_3\text{Sn})_2\text{O}$, *c*-Hex₃SnOH and hydantoic acid were used as received from commercial sources (*c*-Hex = cyclohexyl). Ph_3SnOH was prepared by alkaline hydrolysis of Ph_3SnCl .⁵ The ^1H NMR spectra were recorded on a VA-EM-390 (90 MHz) spectrometer. The IR spectra were recorded on a Pye–Unicam SP-300S spectrophotometer using

‡ Author to whom all correspondence should be addressed.

CsI optics, and UV spectra on a Shimadzu-240 spectrophotometer. Microanalyses were performed at RSIC, Punjab University, and tin was estimated gravimetrically as SnO_2 .

Syntheses

[$\text{Ph}_3\text{Sn}(\text{O}_2\text{CCH}_2\text{N}(\text{H})\text{C}(\text{O})\text{NH}_2)$]

A 250 ml round-bottomed flask was placed on a heating mantle and fitted with a Dean–Stark apparatus with a double-surface, water-cooled reflux condenser. The entire apparatus was flushed with nitrogen to exclude moisture and the reaction was carried out under nitrogen. Ph_3SnOH (1.4 g, 3.8 mmol), hydantoic acid (0.45 g, 3.8 mmol) and dry benzene (150 ml) were placed in the reaction vessel. The reaction was performed under reflux for 24 h with the water produced being removed azeotropically. The resultant solution was concentrated and left to stand overnight. The white solid that precipitated was filtered off and washed successively with petroleum ether (b.p. 60–80 °C) and chloroform. Recrystallization from methanol solution afforded colourless crystals.

The other compounds were prepared using similar procedures; analytical data are given in Table 1.

Crystallography

Intensity data for colourless crystals were measured at room temperature on a Rigaku AFC6R diffractometer fitted with graphite monochromatized $\text{MoK}\alpha$ radiation, $\lambda = 0.71073 \text{ \AA}$, up to θ_{max} 27.5°, employing the $\omega:2\theta$ scan technique. The data were corrected for Lorentz and polarization effects⁶ and for absorption employing the

DIFABS program.⁷ Of the data measured, those that satisfied the $I \geq 3.0\sigma(I)$ criterion of observability were used in the subsequent analysis. Crystal data are summarized in Table 2.

The structures were solved by direct methods⁸ and each refined by a full-matrix least-squares procedure based on F .⁶ Non-hydrogen atoms were refined with anisotropic thermal parameters and hydrogen atoms were included in the models at their calculated positions (C–H, N–H 0.97 Å) with the following exception: in the refinement of [$\text{c-Hex}_3\text{Sn}(\text{O}_2\text{CCH}_2\text{N}(\text{H})\text{C}(\text{O})\text{NH}_2)$], disorder (high thermal motion) was noted in the cyclohexyl ring C(31)–C(36) with two positions being detected for the C(36) atom; this group was refined with isotropic thermal parameters and hydrogen atoms were not included. Final refinement details [sigma weights: i.e. $1/\sigma^2(F)$], are listed in Table 2; the analysis of variance showed no special features in either case. The crystallographic numbering scheme used is shown in Figs 1 and 2 (drawn with ORTEP⁹) and fractional atomic coordinates are listed in Tables 3 and 4. Other crystallographic details comprising thermal parameters, hydrogen-atom parameters, all bond distance and angles, and tables of observed and calculated structure factors are available on request from one of the authors (ERTT).

Biological studies

The new compounds were screened for their antifungal effectiveness *in vitro* against *Alternaria alternata* (ITCC 3022), a causative organism of brown spot disease of tobacco, leaf spot and fruit rot of brinjal, *Helminthosporium sativum* (ITCC 2684),⁹ causal agent of spot blotch of wheat, *Helminthosporium maydis*

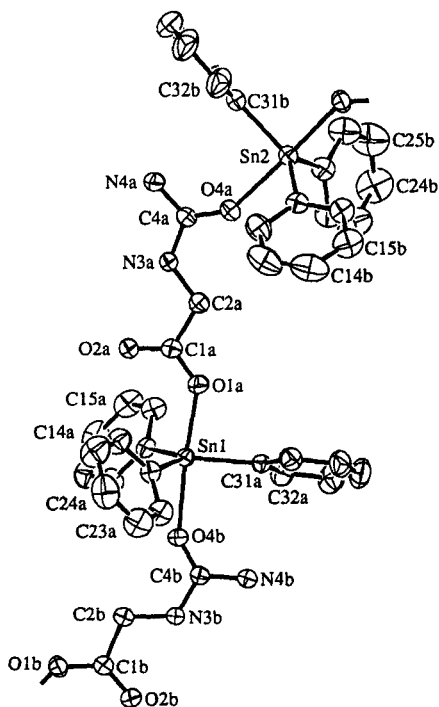
Table 1 Physical data for $\text{R}_3\text{Sn}(\text{O}_2\text{CCH}_2\text{N}(\text{H})\text{C}(\text{O})\text{NH}_2)$

Compound	Yield (%)	M. pt (°C)	λ_{max} (nm) ^a	Elemental analysis (%) ^b			
				C	H	N	Sn
R = Ph ^c	40	203	208	53.8 (54.0)	3.9 (4.3)	5.9 (6.0)	25.3 (25.4)
R = c-Hex ^d	50	194	210	53.7 (52.0)	7.5 (7.8)	6.4 (5.8)	23.9 (24.5)
R = n-Bu ^d	65	112	204	44.4 (44.3)	7.7 (7.9)	7.0 (6.9)	29.1 (29.2)

^a Spectra recorded in methanol solution. ^b Calculated values in parentheses. ^c Recrystallized from methanol solution. ^d Recrystallized from CHCl_3 –petroleum ether (b.p. 60–80 °C) solution.

Table 2 Crystallographic data for $[\text{Ph}_3\text{Sn}(\text{O}_2\text{CCH}_2\text{N}(\text{H})\text{C}(\text{O})\text{NH}_2)]$ (1) and $[\text{c-Hex}_3\text{Sn}(\text{O}_2\text{CCH}_2\text{N}(\text{H})\text{C}(\text{O})\text{NH}_2)]$ (2)

	1	2
Formula	$\text{C}_{21}\text{H}_{20}\text{N}_2\text{O}_3\text{Sn}$	$\text{C}_{21}\text{H}_{38}\text{N}_2\text{O}_3\text{Sn}$
Formula weight	467.1	485.2
Crystal system	Monoclinic	Monoclinic
Space group	$P2_1/n$	$P2_1/n$
a , Å	16.955(6)	10.718(4)
b , Å	14.954(3)	9.088(3)
c , Å	17.865(2)	22.549(6)
β , deg.	115.08(1)	98.49(2)
V , Å ³	4102(1)	2268(1)
Z	8	4
D_{calc} , g cm ⁻³	1.512	1.421
$F(000)$	1872	1008
μ , cm ⁻¹	12.67	11.48
Crystal size, mm	$0.23 \times 0.48 \times 0.48$	$0.08 \times 0.13 \times 0.32$
Transmission coefficients	0.939–1.029	0.870–1.056
No. of data measured	10199	5803
No. of unique data	9879	5517
No. of observed data	6839	3188
R	0.033	0.049
R_w	0.035	0.057
ρ_{max} , e Å ⁻³	0.48	0.88

**Figure 1** A portion of the polymeric structure and crystallographic numbering scheme for $[\text{Ph}_3\text{Sn}(\text{O}_2\text{CCH}_2\text{N}(\text{H})\text{C}(\text{O})\text{NH}_2)]$.

(ITCC 2675),⁹ causal agent of brown spot of maize (*Zea mays*) and *Piricularia oryzae* (ITCC 3050) and a cause of blast disease of rice (*Oryza sativa*). The virulent cultures were obtained from the Plant Pathology Laboratory, Department of Botany, U.N.B. Fungi were grown on potato-dextrose-agar (PDA) medium at $28 \pm 1^\circ\text{C}$.

The fungicidal activities were determined following the spore germination method as described by Rouxel *et al.*¹⁰ Eluents (10 μl) were

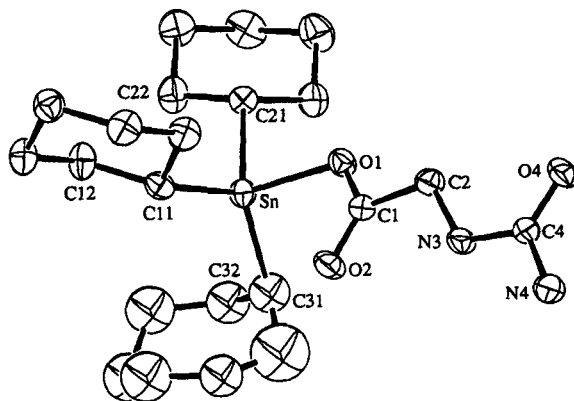


Table 3 Fractional atomic coordinates for $[\text{Ph}_3\text{Sn}(\text{O}_2\text{CCH}_2\text{N}(\text{H})\text{C}(\text{O})\text{NH}_2)]$

Atom	x	y	z
Sn(1)	0.24925(2)	0.12325(2)	0.17665(1)
Sn(2)	0.28465(2)	0.19923(2)	-0.31119(1)
O(1a)	0.2692(2)	0.1617(2)	0.0686(1)
O(1b)	0.2963(2)	0.1506(2)	0.5793(1)
O(2a)	0.2768(2)	0.3111(2)	0.0691(1)
O(2b)	0.2469(2)	0.0101(2)	0.5581(1)
O(4a)	0.2686(2)	0.2565(2)	-0.1981(2)
O(4b)	0.2275(2)	0.0711(2)	0.2887(1)
N(3a)	0.2839(2)	0.3154(2)	-0.0780(2)
N(3b)	0.2453(2)	0.0050(2)	0.4072(2)
N(4a)	0.2924(3)	0.4058(2)	-0.1763(2)
N(4b)	0.2181(3)	-0.0801(2)	0.2945(2)
C(1a)	0.2751(2)	0.2374(2)	0.0382(2)
C(1b)	0.2688(3)	0.0799(2)	0.5368(2)
C(2a)	0.2794(3)	0.2294(2)	-0.0440(2)
C(2b)	0.2649(4)	0.0884(3)	0.4508(2)
C(4a)	0.2808(2)	0.3237(2)	-0.1535(2)
C(4b)	0.2298(3)	0.0009(2)	0.3277(2)
C(11a)	0.1526(2)	0.2204(2)	0.1634(2)
C(11b)	0.3874(3)	0.1216(3)	-0.2230(2)
C(12a)	0.1422(3)	0.2520(3)	0.2319(2)
C(12b)	0.4397(3)	0.1553(3)	-0.1454(3)
C(13a)	0.0788(3)	0.3142(3)	0.2238(3)
C(13b)	0.5035(4)	0.1031(5)	-0.0868(3)
C(14a)	0.0247(3)	0.3452(3)	0.1468(4)
C(14b)	0.5165(4)	0.0178(5)	-0.1049(3)
C(15a)	0.0346(3)	0.3155(3)	0.0789(3)
C(15b)	0.4667(4)	-0.0166(3)	-0.1808(3)
C(16a)	0.0981(3)	0.2538(3)	0.0867(2)
C(16b)	0.4022(3)	0.0351(3)	-0.2402(3)
C(21a)	0.3818(3)	0.1409(2)	0.2602(2)
C(21b)	0.1534(3)	0.1576(3)	-0.3559(2)
C(22a)	0.4232(3)	0.0799(3)	0.3226(3)
C(22b)	0.1215(3)	0.1164(3)	-0.3055(3)
C(23a)	0.5096(3)	0.0899(4)	0.3776(3)
C(23b)	0.0357(4)	0.0839(4)	-0.3374(4)
C(24a)	0.5560(4)	0.1622(4)	0.3706(3)
C(24b)	-0.0171(4)	0.0922(5)	-0.4188(4)
C(25a)	0.5170(4)	0.2228(4)	0.3093(4)
C(25b)	0.0131(4)	0.1320(5)	-0.4701(4)
C(26a)	0.4303(3)	0.2120(3)	0.2535(3)
C(26b)	0.0978(3)	0.1643(4)	-0.4396(3)
C(31a)	0.2050(3)	-0.0019(2)	0.1183(2)
C(31b)	0.3106(3)	0.3296(2)	-0.3423(2)
C(32a)	0.1193(3)	-0.0274(3)	0.0917(3)
C(32b)	0.3921(4)	0.3548(3)	-0.3300(3)
C(33a)	0.0917(4)	-0.1104(4)	0.0563(3)
C(33b)	0.4089(5)	0.4395(4)	-0.3526(4)
C(34a)	0.1485(5)	-0.1674(3)	0.0450(3)
C(34b)	0.3416(7)	0.4980(4)	-0.3883(4)
C(35a)	0.2329(4)	-0.1435(3)	0.0697(3)
C(35b)	0.2607(6)	0.4751(4)	-0.4003(3)
C(36a)	0.2614(3)	-0.0608(3)	0.1064(2)
C(36b)	0.2437(4)	0.3916(3)	-0.3782(3)

placed on two spots 3 cm apart on a clean, grease-free slide and the solvent was allowed to evaporate. One drop of spore suspension (0.02 ml), prepared from 15-day-old culture, was added to the treated spots. In this way sets for various concentrations of the compounds were prepared. The slides were left for 24 h under humid conditions. Finally, one drop of a Cotton Blue–lactophenol mixture was added to each spot to fix the germinated spores. The number of spores germinated compared with the control was calculated, considering an average of 500 spores per treatment. The percentage of inhibition with respect to the control was calculated using the Vincent equation (Eqn [1]):¹¹

$$\text{Inhibition} = \frac{C - T}{T} \times 100\% \quad [1]$$

where C is the number of spores germinated in the control and T is the total number of spores germinated after treatment. The percentage of

Table 4 Fractional atomic coordinates for $[\text{c-Hex}_3\text{Sn}(\text{O}_2\text{CCH}_2\text{N}(\text{H})\text{C}(\text{O})\text{NH}_2)]$

Atom	x	y	z
Sn	0.23034(4)	0.28672(5)	0.11052(2)
O(1)	0.3303(3)	0.1051(5)	0.1479(2)
O(2)	0.4916(4)	0.2549(5)	0.1691(2)
O(4)	0.6864(5)	-0.1946(5)	0.2505(2)
N(3)	0.6393(4)	0.0397(5)	0.2243(2)
N(4)	0.8226(5)	-0.0133(6)	0.2819(3)
C(1)	0.4474(5)	0.1329(7)	0.1679(3)
C(2)	0.5223(5)	-0.0007(7)	0.1897(3)
C(4)	0.7140(6)	-0.0643(7)	0.2518(3)
C(11)	0.3267(5)	0.3339(7)	0.0386(3)
C(12)	0.2353(6)	0.3945(8)	-0.0129(3)
C(13)	0.3039(7)	0.4294(8)	-0.0637(3)
C(14)	0.3718(7)	0.2962(8)	-0.0816(3)
C(15)	0.4613(7)	0.2344(9)	-0.0321(3)
C(16)	0.3968(7)	0.1998(8)	0.0196(3)
C(21)	0.0556(5)	0.1678(7)	0.0874(3)
C(22)	-0.0485(6)	0.2578(9)	0.0517(3)
C(23)	-0.1706(6)	0.1689(9)	0.0372(4)
C(24)	-0.2157(6)	0.1121(10)	0.0899(4)
C(25)	-0.1148(7)	0.0190(9)	0.1252(4)
C(26)	0.0064(6)	0.1082(8)	0.1405(3)
C(31)	0.2111(10)	0.4376(12)	0.1809(4)
C(32)	0.0922(9)	0.5282(12)	0.1740(5)
C(33)	0.0787(12)	0.6250(16)	0.1279(6)
C(34)	0.1717(13)	0.7407(15)	0.1342(6)
C(35)	0.2867(14)	0.6914(16)	0.1308(6)
C(36a) ^a	0.3474(10)	0.5969(13)	0.1723(5)
C(36b) ^a	0.3058(16)	0.5072(21)	0.2051(7)

^a Site occupancy factor = 0.5.

spores inhibited from germination were determined at different concentrations. From these, the effective doses for 50% inhibition, ED_{50} , were calculated in units of $\mu\text{g l}^{-1}$.

Phytotoxicities of the tin compounds were determined on healthy rice seeds of the PUSA-2-21 variety, collected from the Chinsurah Rice Research Institute, Hooghly, West Bengal.

Rice seeds were dipped in suspensions of the compounds of different concentrations (25, 50 and $100 \mu\text{g ml}^{-1}$) for 1, 4 and 8 h. The treated seeds were allowed to germinate sown over a mat of moist filter papers arranged in covered Petri plates. One hundred seeds were treated for each experiment. After seven days the germinated seeds were counted against the control and those seeds which had produced a coleoptile were considered to have germinated. Each experiment was repeated in triplicate. All apparatus and materials were sterilized where necessary, using standard procedures.

RESULTS AND DISCUSSION

Synthesis and spectroscopy

The $\text{R}_3\text{Sn}(\text{O}_2\text{CCH}_2\text{N}(\text{H})\text{C}(\text{O})\text{NH}_2)$ ($\text{R}=\text{Ph}$, *c*-Hex and *n*-Bu) compounds have been prepared in moderate yield from the respective reactions of the triorganotin hydroxides ($\text{R}=\text{Ph}$, *c*-Hex) and oxides ($\text{R}=\text{n-Bu}$) with hydantoic acid; physical data are collected in Table 1.

The ^1H NMR chemical shifts of the resonances, and their integration, observed in the spectra (Table 5) confirm the stoichiometry of the compounds. The assignments of the impor-

tant absorptions in the IR spectra of the new compounds are collected in Table 6. The NH_2 and NH stretching frequencies appear between 3480 and 3120 cm^{-1} in a CsI matrix. The spectra are rather complicated in the region 1650 – 1500 cm^{-1} owing to the presence of amide I, amide II and carboxylate stretching frequencies. Considering hydantoic acid to be a monosubstituted derivative of urea, i.e. $\text{RHNC}(=\text{O})\text{NH}_2$, following the literature precedent,¹² in each case the NH_2 deformation and $\text{C}=\text{O}$ stretching vibrations appear together as very strong, but slightly broad, bands; in solution these split (Table 6). The amide I (CO) in $\text{Ph}_3(\text{O}_2\text{CCH}_2\text{N}(\text{H})\text{C}(\text{O})\text{NH}_2)$ occurs at 1555 cm^{-1} , a clear indication that the $\text{N}-\text{C}(=\text{O})-\text{N}$ carbonyl group is involved in coordination; this is in contrast to the other $\text{R}=\text{c-Hex}$ and $\text{R}=\text{n-Bu}$ derivatives for which the equivalent frequencies occur at 1580 and 1585 cm^{-1} , respectively, in the solid state. The crystal structure determinations of the $\text{R}=\text{Ph}$ and $\text{R}=\text{c-Hex}$ compounds have been undertaken in order to examine in detail the mode of coordination of the hydantoate ligands.

Crystal structures

$[\text{Ph}_3\text{Sn}(\text{O}_2\text{CCH}_2\text{N}(\text{H})\text{C}(\text{O})\text{NH}_2)]$

The structure of $[\text{Ph}_3\text{Sn}(\text{O}_2\text{CCH}_2\text{N}(\text{H})\text{C}(\text{O})\text{NH}_2)]$ is shown in Fig. 1 and selected interatomic parameters are collected in Table 7. The crystallographic asymmetric unit comprises two independent $[\text{Ph}_3\text{Sn}(\text{O}_2\text{CCH}_2\text{N}(\text{H})\text{C}(\text{O})\text{NH}_2)]$ entities, labelled a and b, that do not differ significantly from each other. The structure is polymeric owing to the presence of bridging hydantoate ligands. The carboxylate end of the

Table 5 ^1H NMR data (ppm) for $\text{R}_3\text{Sn}(\text{O}_2\text{CCH}_2\text{N}(\text{H})\text{C}(\text{O})\text{NH}_2)$

Compound	δ (Sn-aromatic/ ligand ring)	δ (NH)	δ (NH_2)	δ (CH_2)	δ (Snn-Bu)	δ (Snc-Hex)
$\text{R}=\text{Ph}^a$	7.96–7.06 (m, 15H)	5.96 (b, 1H)	5.48 (s, 2H)	3.62 (d, 2H, $J=5 \text{ Hz}$)	—	—
$\text{R}=\text{n-Bu}^b$	—	5.06 (t, 1H, $J=5 \text{ Hz}$)	5.02 (s, 2H)	3.97 (d, 2H, $J=5 \text{ Hz}$)	2.20–0.20 (m, 27H)	—
$\text{R}=\text{c-Hex}^b$	—	5.66 (b, 1H)	4.77 (s, 2H)	4.03 (d, 2H, $J=5 \text{ Hz}$)	—	2.30–0.63 (m, 33H)

^a Spectra recorded in saturated solutions of d_6 -DMSO and ^b CDCl_3 solution using internal TMS as reference. All shifts are in ppm downfield to TMS. Proton integrations are in parentheses.

Abbreviations: s, singlet; d, doublet; m, complex multiplet pattern centered at the given δ value; b, broad; t, triplet centred at the given δ value.

Table 6 Selected IR data (cm^{-1}) for $\text{R}_3\text{Sn}(\text{O}_2\text{CCH}_2\text{N}(\text{H})\text{C}(\text{O})\text{NH}_2)$

Compound	$\nu(\text{NH}_2)$	$\nu(\text{NH})$	$\nu(\text{amide II})$ $\nu(\text{NH})$	$\nu(\text{NH}_2)$	$\nu(\text{OCO})$	$\nu(\text{amide I})$ CO	$\nu(\text{SnC})$
R=Ph ^{a, b}	3415 m 3310 m, b	3260 sh, m 3120 w	1525 s	1555 vs, b	1600 s, b	1555 vs, b	280 w 250 w
R=n-Bu ^a	3480 m 3320 m	3300 sh, m 3180 m	1530 vs, b	1585 vs, b	1620 vs	1585 vs, b	480 w 430 w
R=n-Bu ^c	3460 s 3340 s	3100 s, b	1525 s, sh	1565 s, b	1620 vs	1650 vs, b	500 w 470 w
R=c-Hex ^a	3430 m 3340 m	3270 m 3150 m	1525 s, b	1580 vs, b	1615 s, b	1580 vs, b	500 w 470 w
R=c-Hex ^c	3440 m, sh 3380 m, b	3280 m 3230 m	1510 m, b	1565 s	1615 s	1630 s, b	500 w, b 425 w

^a Spectra recorded in CsI optics.^b The solution spectrum of the R=Rh compound was not recorded in solution owing to its poor solubility.^c Spectra recorded in CDCl_3 solution.

Abbreviations: v, very; s, strong; m, medium; w, weak; b, broad; sh, shoulder.

hydantoate anion coordinates a tin atom via one oxygen atom only, whereas the other end coordinates another tin atom via the carbonyl group. The $\text{Sn}(1) \cdots \text{O}(2a)$ and $\text{Sn}(2) \cdots \text{O}(2b)$ separations of 3.544(3) and 3.549(3) Å, respectively, are not representative of significant interactions and the same is true for the $\text{Sn}(1) \cdots \text{N}(4b)$ and $\text{Sn}(2) \cdots \text{N}(4a)$ separations of 3.861(4) and 3.886(3) Å, respectively. The coordination geometry about each tin atom is completed by the *ipso* carbon atoms derived from three phenyl groups which define an equatorial plane in the distorted trigonal-bipyramidal environments about the tin atoms. In this description, the $\text{Sn}(1)$ [$\text{Sn}(2)$] atom lies 0.1093(3) Å [0.0965(3) Å] out of the trigonal plane in the direction of the carboxylate O(1) atom. The Sn–O separations are non-equivalent with the Sn–O(carboxylate) distances of 2.174(2) and 2.174(2) Å, respectively, being significantly shorter than the Sn–O(carbonyl) interactions of 2.319(2) and 2.315(2) Å, respectively; the axial angles are 175.63(8) and 177.4(1)°, respectively. The dihedral angles formed between the three phenyl groups, i.e. C(11–16), C(21–26) and C(31–36), are 93.8, 108.6 and 115.8°, respectively (81.4, 113.6 and 124.6°, respectively for molecule b). In the lattice the polymeric chains are associated via significant hydrogen-bonding contacts. Each of the non-coordinating carbonyl groups forms two $\text{O} \cdots \text{H} \cdots \text{N}$ interactions, such that $\text{O}(2a) \cdots \text{H}(4b1)$ is 2.01 Å (the $\text{O}(2a) \cdots \text{N}(4b)$ separation is 2.901(4) Å and the $\text{O}(2a) \cdots \text{H} \cdots \text{N}(4b)$ angle is 151°) and $\text{O}(2a) \cdots \text{H}(3b)$ is 2.11 Å ($\text{O}(2a) \cdots \text{N}(3b)$ 2.977(4) Å and

$\text{O}(2a) \cdots \text{H} \cdots \text{N}(3b)$ is 148°) and for molecule b, $\text{O}(2b) \cdots \text{H}(4a1)$ is 2.11 Å [symmetry operation: $0.5 - x, -0.5 + y, 0.5 - z$; $\text{O}(2b) \cdots \text{N}(4a)$ is 2.920(4) and $\text{O}(2b) \cdots \text{H} \cdots \text{N}(4a)$ is 140°] and $\text{O}(2b) \cdots \text{H}(3a)$ is 2.19 Å [$\text{O}(2b) \cdots \text{N}(3a)$ is 3.005(4) Å and $\text{O}(2b) \cdots \text{H} \cdots \text{N}(3a)$ is 141°]. The H(4a2) and H(4b2) atoms do not participate in significant hydrogen-bonding contacts. The polymeric structure found for $[\text{Ph}_3\text{Sn}(\text{O}_2\text{CCH}_2\text{N}(\text{H})\text{C}(\text{O})\text{NH}_2)]$ contrasts with the monomeric structure found for the R=c-Hex analogue below.

$[\text{c-Hex}_3\text{Sn}(\text{O}_2\text{CCH}_2\text{N}(\text{H})\text{C}(\text{O})\text{NH}_2)]$

The molecular structure of $[\text{c-Hex}_3\text{Sn}(\text{O}_2\text{CCH}_2\text{N}(\text{H})\text{C}(\text{O})\text{NH}_2)]$ is shown in Fig. 2 and selected interatomic parameters are collected in Table 7. The hydantoate anion coordinates the tin atom via one of the carboxylate oxygen atoms forming a Sn–O(1) interaction of 2.090(4) Å; this separation is shorter than the comparable bonds in the R=Ph derivative. The $\text{Sn} \cdots \text{O}(2)$ separation of 2.948(5) Å is not indicative of a significant interaction between these atoms. The absence of other significant inter- or intramolecular interactions involving the tin atom confirms the monodentate mode of coordination of the hydantoate ligand. The tin atom environment is thus distorted tetrahedral with the maximum distortion from the ideal tetrahedral geometry being manifested in the C(11)–Sn–C(31) angle of 125.6(3) Å which may be traced to the proximity of the non-coordinating O(2) atom. As for the R=Ph derivative there are significant intermolecular hydrogen-bonding

contacts in the lattice, this time involving both the O(2) and O(4) atoms, the latter owing to the non-coordination of this atom to tin; in this structure all three acidic hydrogen atoms participate in hydrogen bonding. The O(2)⋯H(4a) separation is 2.06 Å [symmetry operation: $1.5 - x, 0.5 + y, 0.5 - z$; the O(2)⋯N(4) separation is 3.010(7) Å and the O(2)⋯H—N(4) angle is 168°], O(4)⋯H(4b) is 2.10 Å [symmetry operation: $1.5 - x, -0.5 + y, 0.5 - z$; O(4)⋯N(4) is 2.993(7) Å and O(4)⋯H—N(4)

is 153°] and O(4)⋯H(3) is 2.19 Å [symmetry operation: $1.5 - x, -0.5 + y, 0.5 - z$; O(4)⋯N(3) is 3.058(7) Å and O(4)⋯H—N(3) is 149°].

Hydantoate coordination

The different modes of coordination of the hydantoate ligands in the R=Ph and R=c-Hex structures are reflected in systematic variations of the derived interatomic parameters (Table 7). The ligands in molecules a and b of the R=Ph

Table 7 Selected bond distances (Å) and angles (°) for $R_3Sn(O_2CCH_2N(H)C(O)NH_2)$

Parameter	R=Ph		
	Molecule a	Molecule b	R=c-Hex
Sn—O(1)	2.174(2)	2.174(2) ^a	2.090(4)
Sn—O(4)	2.319(2) ^b	2.315(2) ^c	—
Sn—C(11)	2.127(4)	2.131(4)	2.153(6)
Sn—C(21)	2.122(4)	2.114(5)	2.161(6)
Sn—C(31)	2.118(3)	2.124(4)	2.19(1)
C(1)—O(1)	1.277(4)	1.269(4)	1.299(6)
C(1)—O(2)	1.227(4)	1.222(4)	1.205(7)
C(4)—O(4)	1.243(4)	1.252(4)	1.220(7)
C(2)—N(3)	1.439(4)	1.434(5)	1.438(7)
C(4)—N(3)	1.334(4)	1.331(4)	1.342(7)
C(4)—N(4)	1.334(4)	1.326(4)	1.352(8)
C(1)—C(2)	1.508(5)	1.514(5)	1.503(8)
O(1)—Sn—O(4)	175.63(8) ^b	177.4(1) ^{a,c}	—
O(1)—Sn—C(11)	97.1(1)	97.2(1) ^a	102.3(2)
O(1)—Sn—C(21)	94.3(1)	92.5(1) ^a	94.7(2)
O(1)—Sn—C(31)	87.3(1)	87.9(1) ^a	106.0(3)
O(4)—Sn—C(11)	85.9(1) ^b	85.3(1) ^c	—
O(4)—Sn—C(21)	86.7(1) ^b	86.8(1) ^c	—
O(4)—Sn—C(31)	88.5(1) ^b	90.1(1) ^c	—
C(11)—Sn—C(21)	122.0(1)	121.2(1)	113.6(2)
C(11)—Sn—C(31)	117.0(1)	119.9(2)	125.6(3)
C(21)—Sn—C(31)	120.3(1)	118.2(2)	109.2(3)
Sn—O(1)—C(1)	132.9(2)	131.8(2)	114.0(4)
Sn—O(4)—C(4)	141.7(2) ^{b,d}	143.9(2) ^{c,e}	—
C(2)—N(3)—C(4)	121.5(3)	121.0(3)	120.2(5)
O(1)—C(1)—O(2)	126.7(3)	127.5(3)	122.9(6)
O(1)—C(1)—C(2)	112.8(3)	112.5(3)	114.0(5)
O(2)—C(1)—C(2)	120.5(3)	120.0(3)	123.1(5)
N(3)—C(2)—C(1)	111.9(3)	112.3(3)	111.4(5)
O(4)—C(4)—N(3)	119.8(3)	120.1(3)	123.1(6)
O(4)—C(4)—N(4)	123.7(3)	123.6(3)	122.2(6)
N(3)—C(4)—N(4)	116.5(3)	116.3(3)	114.7(6)
O(1)/C(1)/C(2)/N(3)	178.7(3)	172.0(4)	—165.1(5)
C(1)/C(2)/N(3)/C(4)	—174.2(3)	172.7(4)	174.0(6)
C(2)/N(3)/C(4)/O(4)	4.3(6)	—3.9(7)	—2(1)

^a Atom related by the symmetry operation: $x, y, -1+z$. ^b O(4b).

^c O(4a). ^d C(4b). ^e C(4a).

structure and in the R=c-Hex structure are essentially planar as reflected in the O(1)/C(1)/C(2)/N(3), C(1)/C(2)/N(3)/C(4) and C(2)/N(3)/C(4)/O(4) torsion angles (Table 7). The shorter Sn–O(1) interaction in the R=c-Hex compound leads to a longer C(1)–O(1) bond, i.e. 1.299(6) Å vs 1.277(4) Å (molecule a) and 1.269(4) Å (molecule b) and, concomitantly, shorter C(1)–O(2) interactions, i.e. 1.205(7) Å vs 1.227(4) and 1.222(4) Å, respectively, in the R=Ph structure. Other changes in the ligand parameters relate in particular to the C(4)–N(4) and C(4)–O(4) interactions. The carbonyl C(4)–O(4) bond distance of 1.220(7) Å in the R=c-Hex structure is shorter owing to the non-participation in coordination to tin of this group, in contrast with the situation observed in the R=Ph structure where elongation of this bond is apparent, i.e. 1.243(4) and 1.252(4) Å. As a consequence of the increased bond order of the C(4)–O(4) bond in the R=c-Hex structure, the C(4)–N(4) bond distance is increased [1.352(8) Å] compared with that found in the R=Ph structure [i.e. 1.334(4) and 1.326(4) Å].

General comments

The structure reported here for $[\text{Ph}_3\text{Sn}(\text{O}_2\text{CCH}_2\text{N}(\text{H})\text{C}(\text{O})\text{NH}_2)]$ is similar to those of several other triorganotin carboxylates in which the carboxylate residue contains additional potential donor atoms such as oxygen and nitrogen.^{13,14} The closely related structure $[\text{Ph}_3\text{Sn}(\text{O}_2\text{CCH}_2\text{N}(\text{H})\text{C}(\text{O})\text{NH}_2)]$ ¹⁵ adopts this same motif with important parameters Sn–O(1) 2.143(2), Sn–O(4) 2.352(2) Å and O(1)–Sn–O(4) 171.5(1)°. This motif is similar to that found for many $[\text{R}_3\text{Sn}(\text{O}_2\text{CR}')]$ structures where the carboxylate is bidentate bridging, i.e. the *trans*- R_3SnO_2 motif. The other major structural form found for the $[\text{R}_3\text{Sn}(\text{O}_2\text{CR}')]$ compounds is the isolated, distorted-tetrahedral arrangement as seen in the structure of $[\text{c-Hex}_3\text{Sn}(\text{O}_2\text{CCH}_2\text{N}(\text{H})\text{C}(\text{O})\text{NH}_2)]$.

The observation in the present study of different modes of coordination of the hydantoate ligand leading to disparate structural motifs has many precedents in the structural chemistry of organotin carboxylates. It has been highlighted in recent reviews of the subject that very different structures may be found for closely related chemical formulae.^{13,14} No consistent correlation between steric and/or electronic effects associated with the organotin centre and the nature of the structure adopted ultimately in

Table 8 Effect of the $\text{R}_3\text{Sn}(\text{O}_2\text{CCH}_2\text{N}(\text{H})\text{C}(\text{O})\text{NH}_2)$ compounds on spore germination

Spore	R	ED ₅₀ (mg/ml) ^a
<i>A. alternata</i>	c-Hex	100.00
	Ph	20.00
	n-Bu	0.50
<i>H. aativum</i>	c-Hex	595.60
	Ph	1.42
	n-Bu	0.32
<i>H. maydis</i>	c-Hex	22.40
	Ph	3.55
	n-Bu	0.005
<i>P. oryzae</i>	c-Hex	94.40
	Ph	0.45
	n-Bu	0.005

^a See text.

the solid state has been established yet, however. The presence of multiple potential hydrogen-bonding sites in the hydantoate ligand is another factor that may influence the nature of the structure.¹⁶ It is likely that there is a subtle interplay between all of these factors, as well as the less well-defined crystal packing effects, which is responsible for the observed structural variations. It is also noteworthy that the phenomenon of structural diversity found in the organotin carboxylates is indeed found in other Main Group element systems.^{17,18}

Biocidal activity

The results of the fungitoxicity and phytotoxicity studies are presented in Tables 8 and 9, respec-

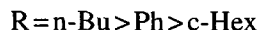
Table 9 Effect of the $\text{R}_3\text{Sn}(\text{O}_2\text{CCH}_2\text{N}(\text{H})\text{C}(\text{O})\text{NH}_2)$ compounds on rice seed germination

R	Concentration (µg/ml)	Percentage of germinated seeds ^a after treatment		
		Duration of treatment		
		1 h	4 h	8 h
c-Hex	100	95	93	90
	50	95	93	93
	25	95	95	94
Ph	100	94	92	91
	50	95	94	94
	25	95	95	95
n-Bu	100	84	81	79
	50	87	83	83
	25	87	85	84
Control		95	95	95

^a With respect to the control.

tively. Rice seed germination studies showed that the R=c-Hex and R=Ph derivatives have practically no phytotoxicity but that the R=n-Bu derivative is more phytotoxic.

From Table 9 it may be seen that the R=n-Bu derivative is the most effective against the fungi used *in vitro*. The funtotoxicities (ED₅₀ values) of the R₃Sn(O₂CCH₂N(H)C(O)NH₂) compounds are in the following order:



Acknowledgements One of us (S.K.K.) is thankful to the University of North Bengal for the award of a Junior Research Fellowship, and the Australian Research Council is thanked for support of the crystallographic facility.

REFERENCES

1. A. J. Crowe, *Appl. Organomet. Chem.* **1**, 143 (1987).
2. A. J. Crowe, *Appl. Organomet. Chem.* **1**, 331 (1987).
3. M. Bergon and J. P. Colmo, *J. Chem. Soc., Perkin Trans II* 193 (1978).
4. A. Chakrabarti, S. K. Kamruddin, T. K. Chattopadhyaya, A. Roy, B. N. Chakraborty, K. C. Molloy and E. R. T. Tiekink, *Appl. Organomet. Chem.* **9**, 357 (1995).
5. R. K. Ingham, S. D. Rosenberg and H. Gilman, *Chem. Rev.* **60**, 459 (1960).
6. teXsan, *Single Crystal Structure Analysis Package*, Molecular Structure Corporation, The Woodlands, TX, 1992.
7. N. Walker and D. Stuart, *Acta Crystallogr., Sect. A* **39**, 158 (1983).
8. G. M. Sheldrick, *SHELXS86, Program for the Automatic Solution of Crystal Structure*, Göttingen, 1986.
9. C. K. Johnson, *ORTEP II*, Report 5136, Oak Ridge National Laboratory, TN, 1976.
10. T. Rouxel, A. Sarniget, A. Kollmann and J. F. Bousquet, *Physiol. Mol. Plant Pathol.* **34**, 507 (1989).
11. J. K. Vincent, *Nature* (London) **159**, 850 (1947).
12. L. J. Bellamy, *The Infrared Spectra of Complex Molecules*, 3rd edn, Vol. 1, Chapman and Hall, London, 1975.
13. E. R. T. Tiekink, *Appl. Organomet. Chem.* **5**, 1 (1991).
14. E. R. T. Tiekink, *Trends Organomet. Chem.* **1**, 71 (1994).
15. K.-M. Lo, V. G. Kumar Das, W.-H. Yip and T. C. W. Mak, *J. Organomet. Chem.* **412**, 21 (1991).
16. S. W. Ng, A. J. Kuthubutheen, V. G. Kumar Das, A. Linden and E. R. T. Tiekink, *Appl. Organomet. Chem.* **8**, 37 (1994).
17. E. R. T. Tiekink, *Main Group Metal Chem.* **15**, 161 (1992).
18. E. R. T. Tiekink and G. Winter, *Rev. Inorg. Chem.* **12**, 183 (1992).